

# Nickel Complexes of Allyl and Vinylidiphenylphosphine

Published as part of the ACS Organic & Inorganic Au virtual special issue “2023 Rising Stars in Organic and Inorganic Chemistry”.

Marissa L. Clapson, David J. Nelson,\* and Marcus W. Drover\*



Cite This: <https://doi.org/10.1021/acsorginorgau.3c00010>



Read Online

ACCESS |



Metrics & More



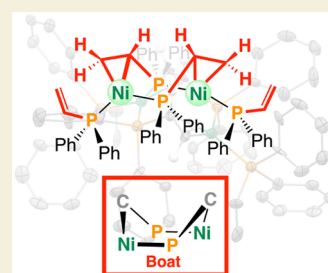
Article Recommendations



Supporting Information

**ABSTRACT:** Monodentate phosphine-ligated nickel compounds, e.g.,  $[\text{Ni}(\text{PPh}_3)_4]$  are relevant as active catalysts across a broad range of reactions. This report expands upon the coordination chemistry of this family, offering the reactivity of allyl- and vinyl-substituted diphenylphosphine ( $\text{PPh}_2\text{R}$ ) with  $[\text{Ni}(\text{COD})_2]$  (COD = 1,5-cyclooctadiene). These reactions provide three-coordinate dinickelacycles that are intermolecularly tethered through adjacent  $\{\text{Ni}\}$ -olefin interactions. The ring conformation of such cycles has been studied in the solid-state and using theoretical calculations. Here, a difference in reaction outcome is linked to the presence of an allyl vs vinyl group, where the former is observed to undergo rearrangement, bringing about challenges in clean product isolation.

**KEYWORDS:** Nickel, Phosphorus, Vinyl, Allyl, Olefin Complexes



## INTRODUCTION

Monodentate phosphine ( $\text{PR}_3$ ) ligands have been central to advancing our understanding of elementary reactivity relevant to nickel catalysis.<sup>1,2</sup> Seminal work on nickel(0) monodentate phosphine complexes led by Kochi and co-workers in the late 1980s contributed greatly to understanding oxidative addition reactions of aryl halide electrophiles—a step that is fundamentally important to cross-coupling.<sup>3</sup> These studies emphasized the importance of ligand design. For example, complexes such as  $[\text{Ni}(\text{PR}_3)_4]$  ( $\text{R} = \text{Et}, \text{Ph}$ ) form equilibrium mixtures of  $[\text{Ni}(\text{PR}_3)_n]$  complexes ( $n = 2, 3, 4$ ) in solution;<sup>1,2,4,5</sup> with the presence of excess  $\text{PR}_3$  ligand attenuating the rate of reaction with electrophiles such as bromobenzene. Here, ligand dissociation is a consequence of cone angle, as  $[\text{Ni}(\text{PMe}_3)_4]$  shows no evidence for ligand dissociation.<sup>6</sup> In this way, there is a balance between ligands that are both sufficiently donating, while also being appropriately bulky, conferring protection or maintaining a desired coordination mode.

Complexes of multidentate phosphine ligands display increased stability in solution (compared to complexes of monodentate counterparts) due to the chelate effect.<sup>7</sup> This has allowed for the development of phosphine donors of variable tether length, cone angle, and donor ability. Recently, our laboratory has brought to light several new diphosphine ligands that feature customized secondary coordination spheres (SCSs) through Lewis acid (boron) incorporation.<sup>8,9</sup> The number of boron moieties in the SCS as well as the length of the alkyl-tethering chain have been shown to affect the coordination chemistry of the resulting nickel species.<sup>10–12</sup> During our investigations on such systems, we have prepared

relevant precursors having pendant allyl or vinyl groups that permit access to boranyl moieties by way of late-stage (post-metal coordination) hydroboration (I, Chart 1A).<sup>12</sup> Such precursor compounds offer rich coordination chemistry in their own regard—an area that capitalizes on the known behavior of  $\pi$ -bonds to serve as  $\sigma$ -donating/ $\pi$ -accepting ligands. As an example,  $[\text{Ni}(\text{PPh}_3)_3]$  readily reacts with ethylene ( $K_{\text{eq}} = 300 \pm 40$ ), to give a three-coordinate adduct,  $[\text{Ni}(\text{PPh}_3)_2(\eta^2\text{-C}_2\text{H}_4)]$  (III, Chart 1A).<sup>6</sup>

In view of the above, we elected to study the reactivity of nickel with two different monodentate phosphine ligands bearing an unsaturated group,  $\text{PPh}_2\text{R}$  ( $\text{R} = \text{allyl or vinyl}$ ), to unearth precursors that could later be hydrofunctionalized, allowing for an examination of potential SCS effects. This study serves as a first step toward that goal, describing the synthesis and characterization of such “ $[\text{Ni}(\text{PPh}_2\text{R})_n]$ ” starting materials. For both  $\text{R} = \text{allyl and vinyl}$ , dinickelacycles are generated, intermolecularly linked by Ni–olefin interactions (Chart 1B). For the allyl variant, phosphine promiscuity is showcased by olefin rearrangement.

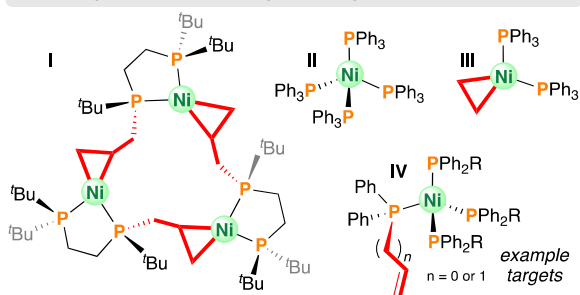
**Received:** March 16, 2023

**Revised:** April 25, 2023

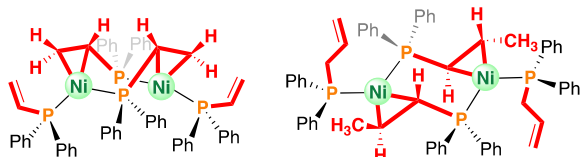
**Accepted:** April 26, 2023

### Chart 1. Nickel Olefin Compounds and Six-Membered Ring Conformations Described Herein

#### A. probing monophosphine ligand design space



#### B. solid-state structures of $\{Ni_2\}$ dimers - vinyl vs. allyl substitution



■ Vinyl group gives  $\{Ni_2\}$  boat ■ Allyl group gives  $\{Ni_2\}$  (E)-crotlyl chair

## RESULTS AND DISCUSSION

### Synthesis of Ni(II) Complexes

*trans*-Nickel(II) dibromo-diphosphine complexes **1** and **2** were synthesized following addition of 2 equiv of either vinyl-diphenylphosphine or allyldiphenylphosphine, respectively, to a THF or  $CH_3CN$  solution of  $NiBr_2$  (Figure 1). Following

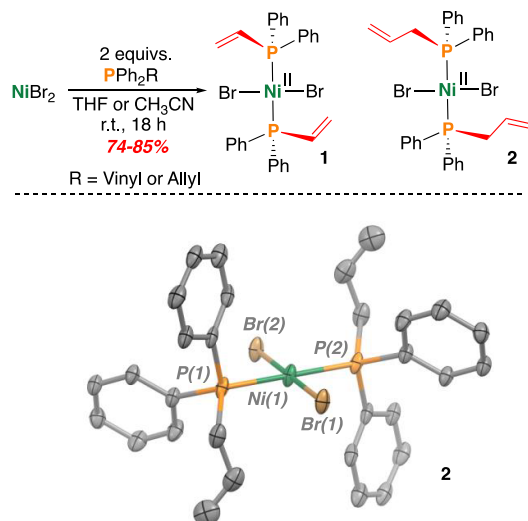


**Figure 1.** Synthesis of  $[Ni^{II}Br_2(PR_3)_2]$  complexes. Inset shows X-ray molecular structure of **2**. Thermal ellipsoids are shown at the 50% probability level. Hydrogen atoms have been omitted for clarity. Selected bond distances (Å) and angles (deg): Ni1–Br1, 2.308(2); Ni1–P1, 2.2342(7); Br1–Ni1–Br2, 180.0; P1–Ni1–P2, 180.0.

workup, the complexes were isolated as green and red solids, respectively. Solutions of **1** and **2** feature broad peaks in their  $^1H$  NMR spectra, consistent with previous reports (Figures S1 and S2).<sup>13–16</sup> Preparative routes for  $[Ni^{II}Br_2(PR_2Vinyl)_2]$ <sup>13</sup> (**1**) and  $[Ni^{II}Br_2(PR_2Allyl)_2]$ <sup>16,17</sup> (**2**) have been reported previously, though the solid-state structure of **2** has not. Accordingly, X-ray quality crystals of **2** were grown by slow

diffusion of pentane into a saturated solution of THF over several days. The nickel center features a square planar geometry, typical of related nickel(II) bis(phosphine) complexes (Figure 1).<sup>14–16</sup> Seeking to next prepare monodentate phosphine nickel(0) compounds, we considered two synthetic routes: (1) direct coordination of allyl or vinyl-diphenylphosphine to a Ni(0) starting material or (2) reduction of the Ni(II) dibromo species **1** or **2**.

### Reactivity of Ni(0) with $PPh_2Vinyl$

As a starting point,  $[Ni(COD)_2]$  was reacted with 4 equiv of vinyl-diphenylphosphine. This reaction, however, did not result in the anticipated compound,  $[Ni(PPh_2Vin)_4]$  akin to  $[Ni(PPh_3)_4]$ , as described above.<sup>4</sup> Analysis by  $^{31}P\{^1H\}$  NMR spectroscopy revealed two broad resonances of relative integration 1:1 at  $\delta_p = 29.1$  and 27.0 ppm, indicative of two inequivalent phosphine environments (Figure S6). The  $^1H$  NMR spectrum of the product additionally showcased two alkene environments, one in which a vinyl group was bound in an  $\eta^2$ -fashion to a Ni(0) center with resonances appearing at  $\delta_H = 3.65$ , 2.75, and 2.21 ppm and a second, in which the vinyl group was unbound, featuring resonances at  $\delta_H = 6.33$ , 5.40, and 5.11 ppm. These resonances were insensitive to temperature (Figure S11, 193–353 K). Together, these data are suggestive of dimer formation, giving  $[Ni(PPh_2CHCH_2)(PPh_2-\eta^2-CHCH_2)]_2$  (**3**). Notably, irrespective of the quantity of vinyl-diphenylphosphine used (2–4 equiv), compound **3** is the only observed product by  $^{31}P\{^1H\}$  NMR spectroscopy.

Reduction of **1** using 2 equiv of cobaltocene ( $Cp_2Co$ ;  $Cp = C_5H_5^-$ ) also produced compound **3** as the sole product (Figure 2). Yellow crystals of **3**, suitable for analysis by X-ray diffraction, corroborated the results observed in solution: a  $[Ni(PPh_2CH_2CH_2)]_2$  dimer connected by two  $\eta^2$ -alkene interactions that self-assemble to produce a six-membered boat-shaped dinickelacycle (Figure 2). The bound  $\eta^2$ -vinyl group features elongated C–C alkene bond lengths of 1.43 Å (taken as an average) and are supported by Ni–C bond lengths of roughly 1.97 Å. The Ni–P bond lengths are equivalent to those in the  $\eta^2$ -bound vinyl-diphenylphosphine moiety featuring a Ni–P bond length of 2.145(2) Å and the unbound with a Ni–P bond length of 2.192(2) Å. This structure can be contrasted with the heavier Pd(I) congener,  $[Pd(PPh_2CHCH_2)(PPh_2-\eta^2-CHCH_2)]_2^{2+}$ , which maintains a very different core structure due to a Pd–Pd interaction ( $d_{Pd-Pd} = 2.748(2)$  Å) (Figure 3).<sup>18</sup>

### Reactivity of Ni(0) with $PPh_2Allyl$

The associated chemistry of  $PPh_2Allyl$  is more convoluted. Reaction of  $[Ni(COD)_2]$  with 4 equiv of allyl diphenylphosphine showcased two broad resonances at  $\delta_p = 18.8$  and  $-1.7$  ppm, consistent with  $[Ni(PPh_2Allyl)_x]$  (cf.  $\delta_p = -16.1$  ppm for free  $PPh_2Allyl$ ). Dynamic behavior of this mixture was observed by variable temperature NMR spectroscopy (Figure S15); fluxionality has also been noted for the related compound,  $[Ni(PPh_2CH_3)_4]$ , which has been ascribed to fast exchange and extensive dissociation.<sup>4</sup> The  $^1H$  NMR spectrum of **4** displays three broad peaks at  $\delta_H = 5.68$ , 4.82, and 2.79 ppm indicative of phosphine coordination to the Ni(0) center without alkene engagement. Furthermore, diffusion ordered  $^1H$  NMR spectroscopy (DOSY)<sup>19</sup> comparing  $[Ni(PPh_2Allyl)_4]$  (**4**) (962 g·mol<sup>-1</sup>) and  $[Ni(PPh_3)_4]$  (1106 g·mol<sup>-1</sup>) displayed similar diffusion coefficients, and therefore hydrodynamic radii, suggestive of similar structures (see the Supporting Information (SI)). Assessing the effect of  $[PR_3]:[Ni]$  ratio, 2–4 equiv

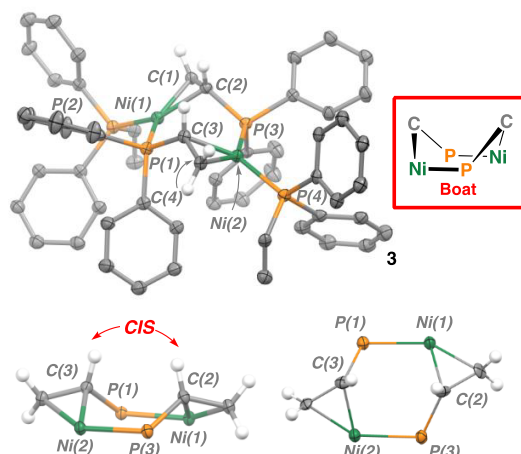
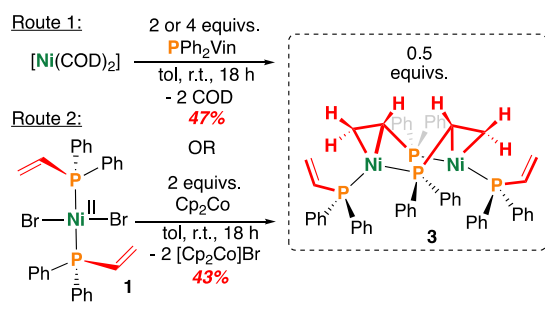


**Figure 2.** Synthesis of a six-membered nickelacycle  $\text{Ni} \eta^2$ -vinyl dimer **3** featuring a boat conformation. Inset shows the X-ray molecular structure depiction of **3** including the core ring structure. Selected bond distances (Å) and angles (deg): Ni1–P1, 2.192(2); Ni1–P2, 2.145(2); Ni2–P3, 2.192(2); Ni2–P4, 2.148(2); Ni1–C1, 1.983(8); Ni1–C2, 1.964(8); Ni2–C3, 1.953(8); Ni2–C4, 1.973(8); P1–Ni1–P2, 115.7(11); C1–Ni1–C2, 42.4(3); P3–Ni2–P4, 116.1(1); C3–Ni2–C4, 42.8(3).

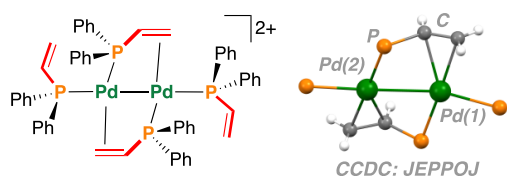


**Figure 3.** Structure of  $[\text{Pd}(\text{PPh}_2\text{CHCH}_2)(\text{PPh}_2\text{-}\eta^2\text{-CHCH}_2)]_2^{2+}$  (CCDC Accession code: JEJPOJ). Adapted from ref 18. Copyright 1990 American Chemical Society.

of allyldiphenylphosphine was added to a solution of  $[\text{Ni}(\text{COD})_2]$ . After the addition of 2 equiv of the phosphine ligand, many signals were observed by  $^{31}\text{P}\{^1\text{H}\}$  NMR spectroscopy, none of which could be confidently assigned as an analogue of **3** (Figure S22); notably, in all of these reactions, downfield-shifted signals ( $\delta_{\text{p}} > 60$  ppm) suggest possible formation of a  $[\text{Ni}]-(\mu\text{-PPh}_2)\text{-}[\text{Ni}]$  unit via P–C(allyl) bond cleavage.<sup>20</sup>

Cooling a reaction mixture of 2 equiv  $\text{PPh}_2\text{Allyl}$  and  $[\text{Ni}(\text{COD})_2]$  in pentane-layered THF at  $-30$  °C over several days deposited some yellow block-like crystals, revealing formation of the dimeric species,  $[\text{Ni}(\text{PPh}_2\text{CH}_2\text{CHCH}_2)(\text{PPh}_2\text{-}\eta^2\text{-CHCHCH}_3)]_2$  (**5**). This compound features one unbound allyl arm, while a second allyl arm has undergone alkene isomerization to give an internal (*E*)-alkene, which coordinates to the Ni(0) center in an  $\eta^2$ -bound fashion, akin to

complex **3** (Figure 4). The shift from a terminal to internal alkene results in the formation of a stable six-membered

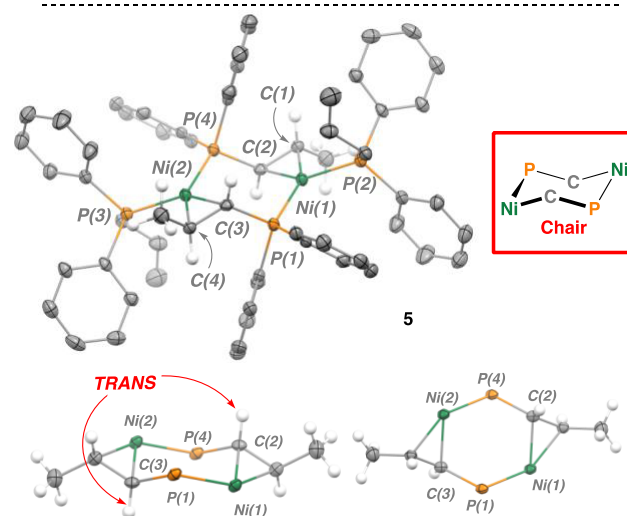
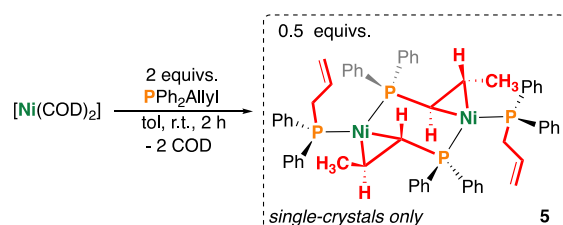


**Figure 4.** Synthesis of a six-membered  $\text{Ni} \eta^2$ -allyl dimer **5**. Inset shows the X-ray molecular structure of **5**. Selected bond distances (Å) and angles (deg): Ni1–P1, 2.1891(9); Ni1–P2, 2.1450(8); Ni2–P3, 2.1450(8); Ni2–P4, 2.1891(9); Ni1–C1, 1.972(3); Ni1–C2, 1.964(3); Ni2–C3, 1.964(3); Ni2–C4, 1.972(3); P1–Ni1–P2, 108.80(4); C1–Ni1–C2, 42.2(1); P3–Ni2–P4, 108.80(4); C3–Ni2–C4, 42.2(1).

dinickelacycle that adopts a chair, rather than boat, configuration. Complex **5** features C–C alkene bond lengths of 1.417(4) Å (C1–C2) and 1.388(4) Å (C4–C5) with an average Ni–C bond length of  $1.967 \pm 0.006$  Å. Interestingly, related allyl dimers have been implicated in the thermal degradation of bis( $\eta^3$ -allyl)nickel complexes, although these have not been characterized.<sup>21</sup> Reductive routes into complex **5** via reduction of **2** using  $\text{Cp}_2\text{Co}$ ,  $\text{KC}_8$ , and Zn have been additionally nonyielding, again resulting in undesired P–C(allyl) bond cleavage, as suggested by  $^{31}\text{P}\{^1\text{H}\}$  NMR spectroscopy (downfield-shifted signals, as noted above).

### Computational Studies

The conformational diversity exhibited by **3** and **5** led us to consider the relative energies of possible six-membered rings (boat vs chair) by computational chemistry (see the SI for details). For vinyl complex **3**, two conformations were considered with the chair being marginally favored by about  $0.7$  kcal mol<sup>−1</sup> (Figure 5); this difference is somewhat negligible, given the anticipated error in such calculations (*ca.*  $0.5$  kcal mol<sup>−1</sup>). For compound **5**, several other conformations are available, owing to (*E/Z*)-boat and -chair configurations. Computational analysis of the boat and chair conformations for the core ring structure of (*E*)-**5** reveal the chair to be the thermodynamic minimum ( $\Delta G^\circ = 6.4$  kcal mol<sup>−1</sup> for the (*E*)-boat conformer), consistent with scXRD



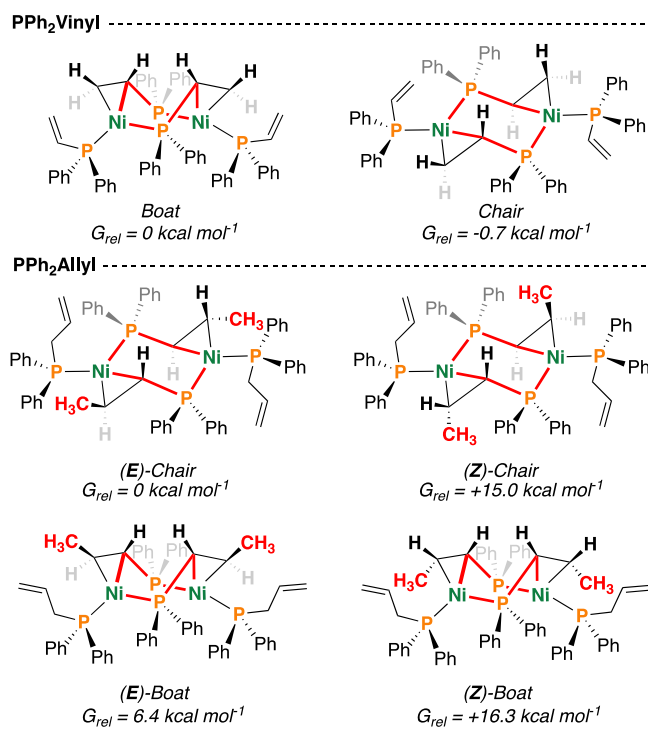


**Figure 5.** Boat and chair ring conformations for  $\{\text{Ni}\}_2$  compounds. Energies calculated using DLPNO-CCSD(T)/cc-pVTZ/SMD (benzene) (see the SI for computational details).

data for **5**. Conformations having a (*Z*)-olefin are higher in energy:  $\Delta G^\circ = 15.0 \text{ kcal mol}^{-1}$  for (*Z*)-chair and  $\Delta G^\circ = 16.3 \text{ kcal mol}^{-1}$  for (*Z*)-boat (Figure 5).

### Initial Hydroboration Reactivity

With complex **3** in hand, we sought to assess whether its six-membered ring-system was amenable to dissociation in the presence of exogenous borane, providing a possible route into  $[\text{Ni}(\text{PR}_3)_2]$ . Consistent with ring retention, addition of 4 equiv of  $\text{HBCy}_2$  to a toluene solution of **3** resulted in a new second order  $^{31}\text{P}\{^1\text{H}\}$  NMR spectrum, with resonances at  $\delta_{\text{P}} = 30.7$  and  $29.2$  ( $J = 22.6, 14.0 \text{ Hz}$ ) (Figure 6). Appearance of a peak at  $\delta_{\text{B}} = 83.4$  in the  $^{11}\text{B}\{^1\text{H}\}$  NMR spectrum confirms the presence of three-coordinate borane moieties, while analysis by  $^1\text{H}$  NMR spectroscopy showed disappearance of the unbound alkene signals and retention of broad  $\eta^2$ -alkene signals at  $\delta_{\text{H}} = 3.56, 2.65,$  and  $2.28 \text{ ppm}$  (like **3**) (Figure S23). This confirms that only the unbound alkene moieties of **3** were hydroborated to give complex **6**, suggesting immunity of the nickel-bound alkenes toward hydroboration-induced ring-opening.

### CONCLUSION

In sum, this report has expanded the space of monodentate phosphine-coordinated nickel chemistry, offering a primary foray into the reactivity of nickel(0) with allyl- and vinyl-diphenylphosphine. Consequently, unique dinickelacycles have been characterized, including by single crystal X-ray diffraction. Reactivity of the vinyl analogue is consistent and predictable, while the converse can be said of its allyl relative. The vinyl compounds are currently the subject of further reactivity investigations that exploit peripheral SCS effects.<sup>23</sup>

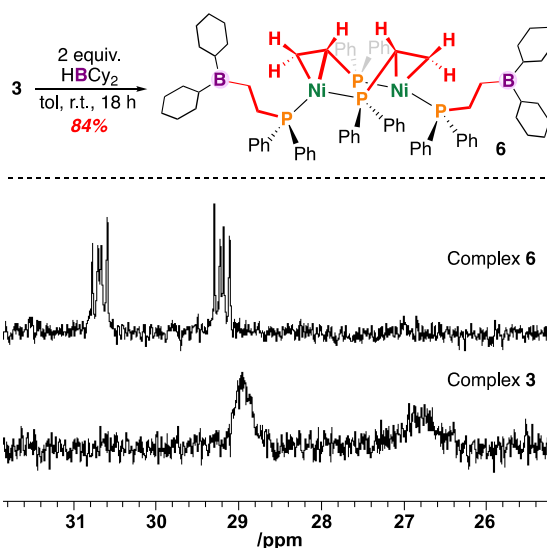


**Figure 6.** Reaction of **3** with  $\text{HBCy}_2$ . Inset shows the  $^{31}\text{P}\{^1\text{H}\}$  NMR spectrum (203 MHz,  $\text{C}_6\text{D}_6$ , 298 K).

## EXPERIMENTAL DATA

### General Considerations

The storage and manipulation of all compounds were carried out under an atmosphere of dry nitrogen either in an MBraun glovebox or employing standard Schlenk techniques under an atmosphere of dry nitrogen. Dried solvents were retrieved from a solvent purification system supplied by PPT, LLC. and stored over molecular sieves. Benzene- $d_6$  was dried over molecular sieves and degassed by three freeze–pump–thaw cycles prior to use.  $\text{HBCy}_2$  was prepared following literature procedures.<sup>22</sup> All other reagents were purchased from commercial vendors and used without further purification unless otherwise stated. All heated experiments were performed using a silicon oil bath unless otherwise stated.

### Physical Methods

NMR spectra were collected on a Bruker Avance III 500 (BBFO probe, TOPSPIN 3.5), Bruker Avance (BBO probe, TOPSPIN 2.1), or 300 MHz Bruker DPX (BBI probe, TOPSPIN 1.3) spectrometer.  $^1\text{H}$  NMR spectra are reported in parts per million (ppm) and are referenced to residual solvent, e.g.,  $^1\text{H}(\text{C}_6\text{D}_6)$ :  $\delta$  7.16;  $^{13}\text{C}(\text{C}_6\text{D}_6)$ : 128.06; coupling constants are reported in Hz.  $^{13}\text{C}$  and  $^{31}\text{P}$  NMR spectra were performed as proton-decoupled experiments and are reported in ppm. For DOSY NMR spectroscopy experiments, the gradient amplitude was varied from 5% to 95% with an optimized  $\delta$  (gradient pulse length) of 1 ms, a spoil gradient of 600  $\mu\text{s}$ , and a  $\Delta$  (diffusion time) of 100 ms. 96 data points were collected in the indirect dimension. Infrared spectra were collected on a Bruker Alpha II FT-IR spectrophotometer with ATR module.

### Compound Preparation

**Synthesis of  $[\text{trans-NiBr}_2(\text{PPH}_2\text{CHCH}_2)_2]$ , **1** [ $\text{C}_{28}\text{H}_{26}\text{Br}_2\text{NiP}_2$ ,  $M_w = 643.0 \text{ g}\cdot\text{mol}^{-1}$ ].** Complex **1** was synthesized following an adapted procedure.<sup>13</sup> To a 100 mL reaction vessel equipped with a Kontes tap was added  $\text{NiBr}_2$  (0.203 g, 0.929 mmol) and suspended in 10 mL of acetonitrile. The reaction solution was heated at  $70^\circ\text{C}$  over 18 h resulting in a blue solution with yellow precipitate. At room temperature, vinyl-diphenylphosphine (0.4 mL, 1.8 mmol) was added dropwise to the reaction solution. The reaction was heated for an additional 18 h at  $50^\circ\text{C}$ . Solvent was removed *in vacuo* and the resulting powder triturated with  $3 \times 2 \text{ mL}$  pentane. The product was dried under vacuum to yield a pale green powder in 85% yield (0.51 g, 0.79 mmol). NMR data are as previously reported.<sup>13</sup>

**Synthesis of  $[\text{trans-NiBr}_2(\text{PPH}_2\text{CH}_2\text{CHCH}_2)_2]$ , **2** [ $\text{C}_{30}\text{H}_{30}\text{Br}_2\text{NiP}_2$ ,  $M_w = 671.0 \text{ g}\cdot\text{mol}^{-1}$ ].** Complex **2** was synthesized following an adapted procedure.<sup>16,17</sup> To a large vial equipped with a

stir bar was added NiBr<sub>2</sub> (0.339 g, 1.55 mmol) and 5 mL of THF. To the reaction solution was added allyldiphenylphosphine (0.67 mL, 3.11 mmol) in a single dose. The reaction was allowed to stir over 18 h becoming dark brown in color. The solution was filtered through a 0.1 μm PTFE syringe filter into a fresh vial and solvent removed *in vacuo*. The resulting residue was triturated with 4 × 1 mL hexanes and dried under vacuum to yield a dark red-brown powder in 74% yield (0.83 g, 1.43 mmol). X-ray quality crystals were grown by slow diffusion of THF and pentane at room temperature over 5 days—the crystal structure of **2** has not been reported and is thus provided here. NMR data are as previously reported.<sup>16,17</sup>

**Synthesis of [Ni(PPH<sub>2</sub>CHCH<sub>2</sub>)(PPH<sub>2</sub>-η<sup>2</sup>-CHCH<sub>2</sub>)<sub>2</sub>]<sub>2</sub>, **3** [C<sub>56</sub>H<sub>52</sub>Ni<sub>2</sub>P<sub>4</sub>, Mw = 966.3 g·mol<sup>-1</sup>]. **Method 1:** In a large vial equipped with a stir bar, [Ni(COD)<sub>2</sub>] (0.054 g, 0.20 mmol) was dissolved in 5 mL of toluene. To the reaction was added vinylidiphenylphosphine (0.13 mL, 0.65 mmol) in a single dose. The reaction became bright orange in color and was allowed to stir over 18 h at room temperature. Solvent was removed *in vacuo* and the resulting orange residue triturated with 4 × 2 mL pentane and dried under vacuum to yield a fluffy bright yellow powder in 47% yield (0.084 g, 0.093 mmol). X-ray quality crystals were grown by slow evaporation of THF at room temperature over 3 days. **Method 2:** To a large vial equipped with a stir bar was added **1** (0.101 g, 0.157 mmol) alongside Cp<sub>2</sub>Co (0.062 g, 0.33 mmol) and dissolved in 3 mL toluene. The reaction was allowed to stir over 18 h resulting in a brown solution with yellow-brown precipitate. The toluene solution was filtered through a 0.1 μm PTFE syringe filter into a fresh 20-dram vial and solvent removed *in vacuo*. The resulting residue was triturated with 3 × 1 mL pentane and dried under vacuum to yield a yellow/brown powder in 43% yield (0.065 g, 0.067 mmol). Potassium graphite (KC<sub>8</sub>) can likewise be used as the reducing agent under the same reaction conditions using THF as the reaction solvent. <sup>1</sup>H NMR (500 MHz, C<sub>6</sub>D<sub>6</sub>) δ<sub>H</sub>: 8.01 (m, 4H, Ar-H), 7.84 (m, 4H, Ar-H), 7.40 (m, 4H, Ar-H), 7.30 (m, 4H, Ar-H), 7.11–6.88 (m, 24H, Ar-H), 6.33 (m, 2H, CH=CH<sub>2</sub>), 5.40 (m, 2H, CH=CH<sub>2</sub>), 5.11 (m, 2H, CH=CH<sub>2</sub>), 3.65 (m, 2H, Ni-η<sup>2</sup> CH=CH<sub>2</sub>), 2.75 (m, 2H, Ni-η<sup>2</sup> CH=CH<sub>2</sub>), 2.21 (m, 2H, Ni-η<sup>2</sup> CH=CH<sub>2</sub>). <sup>13</sup>C{<sup>1</sup>H} NMR (126 MHz, C<sub>6</sub>D<sub>6</sub>) δ<sub>C</sub>: 137.0 (Ar-CH), 136.5 (Ar-CH), 134.4 (m), 133.9 (m), 133.5 (d, J = 12.8 Hz), 133.3 (d, J = 12.8 Hz), 53.0 (s, Ni-η<sup>2</sup> CH=CH<sub>2</sub>), 47.7 (s, Ni-η<sup>2</sup> CH=CH<sub>2</sub>). \*Other (sp<sup>2</sup>-C) signals overlap with the solvent signal. <sup>31</sup>P{<sup>1</sup>H} NMR (203 MHz, C<sub>6</sub>D<sub>6</sub>) δ<sub>P</sub>: 29.1 (br), 27.0 (br). DOSY<sup>1</sup>H NMR (500 MHz, C<sub>6</sub>D<sub>6</sub>): D = 5.11 × 10<sup>-10</sup> m<sup>2</sup>·s<sup>-1</sup>.**

**Synthesis of [Ni(PPH<sub>2</sub>CH<sub>2</sub>CHCH<sub>2</sub>)<sub>4</sub>]<sub>2</sub>, **4** [C<sub>60</sub>H<sub>60</sub>NiP<sub>4</sub>, Mw = 963.7 g·mol<sup>-1</sup>]. In a large vial equipped with a stir bar [Ni(COD)<sub>2</sub>] (0.052 g, 0.19 mmol) was dissolved in 2 mL of toluene. To the reaction was added allyldiphenylphosphine (0.16 mL, 0.74 mmol) in a single dose. The reaction became dark red in color and was allowed to stir over 18 h at room temperature. Solvent was removed *in vacuo* and the resulting dark red residue triturated with 3 × 2 mL pentane and dried under vacuum to yield a sticky red solid in 74% yield (0.14 g, 0.14 mmol). <sup>1</sup>H NMR (500 MHz, C<sub>6</sub>D<sub>6</sub>) δ<sub>H</sub>: 7.38 (m, 16H, Ar-H), 7.12–6.96 (m, 24H, Ar-H), 5.68 (br, 4H, CH=CH<sub>2</sub>), 4.89–4.74 (br, 8H, CH=CH<sub>2</sub>), 2.79 (br, 8H, P-CH<sub>2</sub>-CH=CH<sub>2</sub>). <sup>13</sup>C NMR (126 MHz, C<sub>6</sub>D<sub>6</sub>) δ<sub>C</sub>: 138.7 (m, Ar-C), 133.4 (s, Ar-CH), 133.35 (br, Ar-H), 128.5 (s, Ar-CH), 116.7 (br, CH=CH<sub>2</sub>), 35.3 (br, P-CH<sub>2</sub>). Additional aromatic carbon and allyl(CH) signals are obscured by benzene solvent signal. <sup>31</sup>P{<sup>1</sup>H} NMR (203 MHz, C<sub>6</sub>D<sub>6</sub>) δ<sub>P</sub>: 18.8 (br, Δ<sub>1/2</sub> = 571 Hz), -1.7 (br). DOSY<sup>1</sup>H NMR (500 MHz, C<sub>6</sub>D<sub>6</sub>): D = 7.90 × 10<sup>-10</sup> m<sup>2</sup>·s<sup>-1</sup> cf. D = 7.35 × 10<sup>-10</sup> m<sup>2</sup>·s<sup>-1</sup> for [Ni(PPH<sub>3</sub>)<sub>4</sub>].**

**Synthesis of [Ni(PPH<sub>2</sub>CH<sub>2</sub>CHCH<sub>2</sub>)(PPH<sub>2</sub>-η<sup>2</sup>-CHCHCH<sub>3</sub>)<sub>2</sub>]<sub>2</sub>, **5** [C<sub>90</sub>H<sub>90</sub>Ni<sub>2</sub>P<sub>6</sub>, Mw = 1474.9 g·mol<sup>-1</sup>]. In a large vial equipped with a stir bar [Ni(COD)<sub>2</sub>] (0.050 g, 0.18 mmol) was added and dissolved in toluene. To the reaction mixture was added allyldiphenylphosphine (0.08 mL, 0.36 mmol) dropwise, becoming dark red in color. The reaction was allowed to stir for 2 h before solvent was removed *in vacuo*, and the resulting residue triturated with 3 × 1 mL pentane resulting in a red powder. The red powder (0.066 g) was dissolved in minimal THF, layered with pentane, and placed in**

the freezer at -30 °C over 5 days, resulting in some yellow crystals of the (E)-crotyl dimer, suitable for analysis by X-ray crystallography.

**Synthesis of Ni<sub>2</sub>(PPH<sub>2</sub>CH<sub>2</sub>CH<sub>2</sub>BCy<sub>2</sub>)<sub>2</sub>(PPH<sub>2</sub>-η<sup>2</sup>-CHCH<sub>2</sub>)<sub>2</sub>, **6** [C<sub>80</sub>H<sub>98</sub>B<sub>2</sub>Ni<sub>2</sub>P<sub>4</sub>, Mw = 1322.57 g·mol<sup>-1</sup>]. In a large vial equipped with a stir bar, **3** (0.047 g, 0.049 mmol) was dissolved in 2 mL of toluene. To the reaction was added HBCy<sub>2</sub> (0.022 g, 0.12 mmol) in a single dose. The reaction became orange/yellow in color and was allowed to stir over 18 h at room temperature. Solvent was removed *in vacuo* and the resulting brown residue triturated with 3 × 1 mL pentane and dried under vacuum to yield a fluffy bright yellow powder in 84% yield (0.054 g, 0.041 mmol). <sup>1</sup>H NMR (500 MHz, C<sub>6</sub>D<sub>6</sub>) δ<sub>H</sub>: 8.01 (m, 4H, Ar-H), 7.90 (m, 4H, Ar-H), 7.41 (m, 4H, Ar-H), 7.33 (m, 4H, Ar-H), 7.15–7.00 (m, 24H, Ar-H), 3.56 (m, 2H, Ni-η<sup>2</sup> CH=CH<sub>2</sub>), 2.65 (m, 2H, Ni-η<sup>2</sup> CH=CH<sub>2</sub>), 2.28 (m, 2H, Ni-η<sup>2</sup> CH=CH<sub>2</sub>), 2.15 (m, 4H), 1.68 (m, 10H, CH<sub>2</sub>/CH), 1.41–1.10 (m, 30H, CH<sub>2</sub>/CH), 0.99–0.83 (m, 8H, CH<sub>2</sub>/CH). <sup>13</sup>C{<sup>1</sup>H} NMR (125 MHz, C<sub>6</sub>D<sub>6</sub>) δ<sub>C</sub>: 138.7 (Ar-CH), 138.5 (Ar-CH), 134.9 (m), 134.2 (m), 133.3 (d, J = 12.8 Hz), 133.2 (d, J = 12.8 Hz), 53.1 (s, Ni-η<sup>2</sup> CH=CH<sub>2</sub>), 45.6 (s, Ni-η<sup>2</sup> CH=CH<sub>2</sub>), 36.0 (s), 30.2 (br), 27.8 (s), 27.33 (s), 27.32 (s). \*Other (sp<sup>2</sup>-C) signals overlap with the solvent signal. <sup>31</sup>P{<sup>1</sup>H} NMR (203 MHz, C<sub>6</sub>D<sub>6</sub>) δ<sub>P</sub>: 30.7 (dd, J = 22.3, 14.0 Hz), 29.2 (dd, J = 22.6, 14.0 Hz). <sup>11</sup>B NMR (161 MHz, C<sub>6</sub>D<sub>6</sub>) δ<sub>B</sub>: 83.4.**

## ■ ASSOCIATED CONTENT

### Data Availability Statement

The data underlying this study are available in the published article and its Supporting Information.

### Supporting Information

The Supporting Information is available free of charge at <https://pubs.acs.org/doi/10.1021/acsorginorgau.3c00010>.

<sup>1</sup>H, <sup>13</sup>C{<sup>1</sup>H}, <sup>31</sup>P{<sup>1</sup>H}, and <sup>11</sup>B NMR spectra for all complexes (PDF)

XYZ coordinates for DFT calculations (XYZ)

### Accession Codes

CCDC 2245379–2245381 contain the supplementary crystallographic data for this paper. These data can be obtained free of charge via [www.ccdc.cam.ac.uk/data\\_request/cif](http://www.ccdc.cam.ac.uk/data_request/cif), or by emailing [data\\_request@ccdc.cam.ac.uk](mailto:data_request@ccdc.cam.ac.uk), or by contacting The Cambridge Crystallographic Data Centre, 12 Union Road, Cambridge CB2 1EZ, UK; fax: +44 1223 336033.

## ■ AUTHOR INFORMATION

### Corresponding Authors

David J. Nelson – WestCHEM Department of Pure and Applied Chemistry, University of Strathclyde, Glasgow G1 1XL, Scotland, U.K.; [orcid.org/0000-0002-9461-5182](https://orcid.org/0000-0002-9461-5182); Email: [david.nelson@strath.ac.uk](mailto:david.nelson@strath.ac.uk)

Marcus W. Drover – Department of Chemistry and Biochemistry, The University of Windsor, Windsor, ON N9B 3P4, Canada; [orcid.org/0000-0002-2186-1040](https://orcid.org/0000-0002-2186-1040); Email: [mdrover@uwindsor.ca](mailto:mdrover@uwindsor.ca)

### Author

Marissa L. Clapson – Department of Chemistry and Biochemistry, The University of Windsor, Windsor, ON N9B 3P4, Canada

Complete contact information is available at:

<https://pubs.acs.org/doi/10.1021/acsorginorgau.3c00010>

## Author Contributions

CRedit: **Marissa L. Clapson** formal analysis (supporting), investigation (lead), methodology (supporting), writing-original draft (supporting), writing-review & editing (supporting); **David James Nelson** conceptualization (equal), formal analysis (equal), funding acquisition (equal), investigation (equal), methodology (equal), writing-review & editing (equal); **Marcus W. Drover** conceptualization (equal), data curation (lead), formal analysis (lead), funding acquisition (lead), methodology (lead), project administration (lead), supervision (lead), validation (lead), writing-original draft (lead), writing-review & editing (lead).

## Notes

The authors declare no competing financial interest.

## ACKNOWLEDGMENTS

The authors are grateful to the University of Windsor, the Council of Ontario Universities for a John C. Polanyi award to M.W.D., the Natural Sciences and Engineering Research Council of Canada (Discovery Grant, RGPIN-2020-04480, Discovery Launch Supplement, DGEGR-2020-00183), donors of the American Chemical Petroleum Research Fund (PRF # 62284-ND3), and the Canadian Foundation for Innovation (Project # 41099). D.J.N. thanks the Carnegie Trust for the Universities of Scotland for a Research Incentive Grant (RIG008165). Some of the calculations were performed using the Archie-WEST High-Performance Computer ([www.archie-west.ac.uk](http://www.archie-west.ac.uk)) at the University of Strathclyde; we thank Mr J. Buzzard, Dr K. Kubiak-Ossowska, and Dr R. Martin for their assistance with this facility. We thank Prof. Louise N. Dawe (Wilfrid Laurier University) for helpful discussions relevant to crystallography.

## REFERENCES

- (1) Ananikov, V. P. Nickel: The "Spirited Horse" of Transition Metal Catalysis. *ACS Catal.* **2015**, *5* (3), 1964–1971.
- (2) Greaves, M. E.; Johnson Humphrey, E. L. B.; Nelson, D. J. Reactions of Nickel(0) with Organochlorides, Organobromides, and Organoiodides: Mechanisms and Structure/Reactivity Relationships. *Catal. Sci. Technol.* **2021**, *11* (9), 2980–2996.
- (3) Tsou, T. T.; Kochi, J. K. Mechanism of Oxidative Addition. Reaction of Nickel(0) Complexes with Aromatic Halides. *J. Am. Chem. Soc.* **1979**, *101* (21), 6319–6332.
- (4) Tolman, C. A.; Seidel, W. C.; Gosser, L. W. Formation of Three-Coordinate Nickel(0) Complexes by Phosphorus Ligand Dissociation from NiL<sub>4</sub>. *J. Am. Chem. Soc.* **1974**, *96* (1), 53–60.
- (5) Dalton, J.; Föi, B. M.; Cassar, L.; Ricerche Donegani, I. G.; Gerlach, D. H.; Kane, A. R.; Parshall, G. W.; Jesson, J. P.; Muetterties, E. L.; Hidai, M.; Rashiwagi, T.; Ireuchi, T.; Uchida, Y. Oxidative Addition of Aryl Halides to Tris(Triphenylphosphine)Nickel(0). *J. Chem. Soc., Dalton Trans.* **1975**, *7* (23), 2572–2576.
- (6) Tolman, C. A.; Seidel, W. C.; Gerlach, D. H. Triarylphosphine and Ethylene Complexes of Zerovalent Nickel, Palladium, and Platinum. *J. Am. Chem. Soc.* **1972**, *94* (8), 2669–2676.
- (7) Lundgren, R. J.; Stradiotto, M. Key Concepts in Ligand Design. In *Ligand Design in Metal Chemistry*; John Wiley & Sons, Ltd: Chichester, UK, 2016.
- (8) Zurakowski, J. A.; Austen, B. J. H.; Drover, M. W. Exterior Decorating: Lewis Acid Secondary Coordination Spheres for Cooperative Reactivity. *Trends Chem.* **2022**, *4* (4), 331–346.
- (9) Drover, M. W. A Guide to Secondary Coordination Sphere Editing. *Chem. Soc. Rev.* **2022**, *51* (6), 1861–1880.
- (10) Drover, M. W.; Dufour, M. C.; Lesperance-Nantau, L. A.; Noriega, R. P.; Levin, K.; Schurko, R. W. Octaboraneyl Complexes of Nickel: Monomers for Redox-Active Coordination Polymers. *Chem.-Eur. J.* **2020**, *26* (49), 11180–11186.
- (11) Austen, B. J. H.; Sharma, H.; Zurakowski, J. A.; Drover, M. W. Racemic and Meso Diastereomers of a P-Chirogenic Diboranyldi-phosphinoethane. *Organometallics* **2022**, *41* (19), 2709–2715.
- (12) Clapson, M.; Sharma, H.; Zurakowski, J.; Drover, M. W. Cooperative Nitrile Coordination Using Nickel and a Boron-Containing Secondary Coordination Sphere. *Chem.-Eur. J.* **2023**, *29*, e202203763.
- (13) Que, L.; Pignolet, L. H. Proton Magnetic Resonance Study of the Stereochemistry of Four-Coordinate Nickel(II) Complexes. Dihalobis(Tertiary Phosphine)Nickel(II) Complexes. *Inorg. Chem.* **1973**, *12* (1), 156–163.
- (14) Coles, S. J.; Faulds, P.; Hursthouse, M. B.; Kelly, D. G.; Ranger, G. C.; Walker, N. M. Synthesis and Characterisation of Nickel(II) Diphenylalkenylphosphine Complexes. *J. Chem. Res.* **1999**, *7*, 418–419.
- (15) Corain, B.; Longato, B.; Angeletti, R.; Valle, G. Trans-[Dichlorobis(Triphenylphosphine)Nickel(II)](C<sub>2</sub>H<sub>4</sub>Cl<sub>2</sub>)<sub>2</sub>: A Clathrate of the Allogon of Venanzi's Tetrahedral Complex. *Inorg. Chim. Acta* **1985**, *104* (1), 15–18.
- (16) Hyder, I.; Jiménez-Tenorio, M.; Puerta, M. C.; Valerga, P. Oligomerization and Regioselective Hydrosilylation of Styrenes Catalyzed by Cationic Allyl Nickel Complexes Bearing Allylphosphine Ligands. *Dalton Trans.* **2007**, 3000–3009.
- (17) Browning, M. C.; Mellor, J. R.; Morgan, D. J.; Pratt, S. A. J.; Sutton, L. E.; Venanzi, L. M. 134. Tetrahedral Complexes of Nickel(II) and the Factors Determining Their Formation. Part IV. Complexes with Tribenzyl-, Dibenzylphenyl-, Benzylidiphenyl-, and Allyldiphenyl-Phosphine. *J. Chem. Soc.* **1962**, 693–703.
- (18) Wilson, W. L.; Nelson, J. H.; Alcock, N. W. Facile Synthesis and Structural Characterization of [(Ph<sub>2</sub>PCHCH<sub>2</sub>)(μ-η<sup>3</sup>-Ph<sub>2</sub>PCHCH<sub>2</sub>)Pd<sup>II</sup>]<sub>2</sub>(BF<sub>4</sub>)<sub>2</sub>: Unprecedented Formation of a Structurally Unusual Palladium(I) Complex. *Organometallics* **1990**, *9* (5), 1699–1700.
- (19) Evans, R.; Dal Poggetto, G.; Nilsson, M.; Morris, G. A. Improving the Interpretation of Small Molecule Diffusion Coefficients. *Anal. Chem.* **2018**, *90* (6), 3987–3994.
- (20) Touchton, A. J.; Wu, G.; Hayton, T. W. Generation of a Ni<sub>3</sub> Phosphinidene Cluster from the Ni(0) Synthone, Ni(η<sup>3</sup>-CPh<sub>3</sub>)<sub>2</sub>. *Organometallics* **2020**, *39* (8), 1360–1365.
- (21) Flid, V. R.; Zamalyutin, V. V.; Shamsiev, R. S.; Katsman, E. A. Kinetics and Mechanism of Thermal Decomposition of Bis(η<sup>3</sup>-Allyl) Nickel Complexes. *Kinet. Catal.* **2019**, *60* (2), 113–117.
- (22) Abiko, A. Dicyclohexylboron Trifluoromethanesulfonate. *Org. Synth.* **2003**, *79*, 103.
- (23) This work was deposited on ChemRxiv: Clapson, M. L.; Nelson, D. N.; Drover, M. W. Nickel Complexes of Allyl and Vinylidiphenylphosphine. *ChemRxiv*, March 17, 2023, ver. 1. DOI: [10.26434/chemrxiv-2023-cvmhj](https://doi.org/10.26434/chemrxiv-2023-cvmhj).